

Anomalous phospholipid subdiffusion in compartmentalized cell membrane and the mathematical model of the time-dependent diffusion coefficient

Paulius Miškinis

*Department of Physics, Faculty of
Fundamental Sciences, Vilnius Gediminas
Technical University, Saulėtekio Ave. 11,
LT-10223, Vilnius-40, Lithuania*

Recent experimental data on an anomalous diffusion of phospholipids in compartmentalized cell membrane are analysed. A new mathematical model of passive transport with the time-dependent diffusion coefficient is proposed. The model with the step-type asymptotical dependence of the diffusion coefficient is applied to a concrete example, and a correspondence between the experimental and theoretical results is shown. The random distribution of immobilized obstructions as well as the membrane skeleton meshwork offer a theoretical basis for modifying the available models of transport and thus for refining the diffusion model. The experimentally obtained time-dependent coefficient of diffusion is shown to agree with the proposed theoretical model.

Key words: passive transport, the first Fick's law, mathematical modeling

INTRODUCTION

Many cellular processes, such as signaling, involve the interaction of several individual molecules that must come together to transmit information across the plasma membrane to the cell interior.

Recently, membrane molecules have been shown to undergo anomalous subdiffusion (see [1–4] and ref. therein). Unlike the simple Brownian diffusion, which is isotropic and homogeneous, anomalous diffusion may be anisotropic on some time-scales. In the case of anomalous subdiffusion, the timescale of the measurement becomes intimately and nontrivially related to the observed motion.

Anomalous subdiffusion most likely is a result of two main mechanisms that act on the molecules of the membrane simultaneously. The first has been shown by M. J. Saxton [5]: a random distribution of immobilized obstructions is sufficient to produce anomalous subdiffusion at scales shorter than the length characteristic of the average cluster size of obstacles.

The second mechanism relates with temporary confinement of the diffusing protein. Also, experimental evidence, from both single particle tracking [6, 7] and optical-tweezers-based molecular dragging studies [8, 9], implies that the cytoplasmic portion of transmembrane proteins nonspecifically collides with the membrane skeleton, causing temporary confinement of the diffusing protein in compartments formed by the membrane skeleton meshwork. This results in so-called hop diffusion where free diffusion occurs inside compartments with infrequent intercompartmental transitions. At timescales intermediate to the tracer

sensing the compartment boundaries and the average residency time in a compartment, anomalous diffusion is observed.

In this paper, the experimental data on hop diffusion are analysed employing the mathematical time-dependent diffusion coefficient model, and the correspondence between the experimental and theoretical results is discussed.

EXPERIMENTAL DATA

Cell culture. PtK2 kangaroo rat kidney cells were grown in Eagle's Minimum Essential Medium supplemented with 10% fetal bovine serum. Cells were plated on 18 × 18 mm coverslips (for high-speed video imaging) or 12-mm diameter glass-based dishes (for single fluorescent-molecule video imaging) obtained from Matsunami (Kishiwada, Japan) and Iwaki (Funabashi, Japan), respectively, and used 2–3 days later.

Gold probe preparation and fluorescent probe labeling. Colloidal gold particles 40-nm in diameter (BB International, Cardiff, UK) were conjugated with bovine holo transferrin (Wako, Osaka, Japan). The amount of transferrin mixed with the gold particles was varied to minimize the effect of crosslinking by the gold probe [3]. For single fluorescent-molecule video imaging, transferrin was labeled with Alexa555-succinimide (Molecular Probes, Eugene, OR). Before observation, cells were incubated in a transferrin-free medium for 15 min at 37 °C, washed, and then a gold probe or fluorescent probe was applied at 37 °C.

Total internal reflection fluorescence microscopy. Single fluorescent-molecule video imaging was performed on a home-built objective-lens-type total internal fluorescence microscope using a 1.45 NA TIRF objective (Olympus, Tokyo, Japan) [3, 10]. Imaging was performed through an image intensifier (Model # C8600-03, Hamamatsu Photonics, Hamamatsu City, Japan)

coupled to a EB-CCD camera (Model # C7190-23, Hamamatsu Photonics). Camera output was stored on DV tape (Model # DSR-20, Sony, Tokyo, Japan) for post-experiment tracking.

High-speed video microscopy. High-speed video microscopy was carried out as described previously [3, 6]. The precision of the position determination was estimated from the standard deviation of the coordinates of 40-nm diameter gold particles attached to a poly-L-lysine-coated coverslip, further covered with a 10% polyacrylamide gel, and was 17 nm and 6.9 nm at time-resolutions of 25 μ s and 2 ms, respectively. On the same instrumental setup, Murase et al. [2] found the precision to be 13 nm at a time-resolution of 25 μ s for gold-labeled fluorescein-DOPE incorporated in large, unilamellar vesicles in the gel phase at 25 °C. This result is comparable to that for gold particles attached on the coverslip. Thus, the limiting factor in the position determination in these experiments using immobilized gold particles at the varying exposure times is most likely the signal/noise ra-

tio in the image of the particle. The positional resolution begets a limit on the smallest diffusion coefficient that may be measured. At a time-resolution of 25 μ s, the smallest measurable diffusion coefficient was found to be 0.021 μ m²/s (Murase et al., [2]).

Total internal reflection fluorescence microscopy. Single fluorescent-molecule video imaging was performed on a home-built objective-lens-type total internal fluorescence microscope using a 1.45 NA TIRF objective (Olympus, Tokyo, Japan) [3, 10]. Imaging was performed through an image intensifier (Model # C8600-03, Hamamatsu Photonics, Hamamatsu City, Japan) coupled to a EB-CCD camera (Model # C7190-23, Hamamatsu Photonics). Camera output was stored on DV tape (Model # DSR-20, Sony, Tokyo, Japan) for post-experiment tracking.

The experimental plot of the mean squared displacement (MSD) of granules as a function of time in various time scales and the time-dependence of the diffusion coefficient D is shown in Fig. 1 [1].

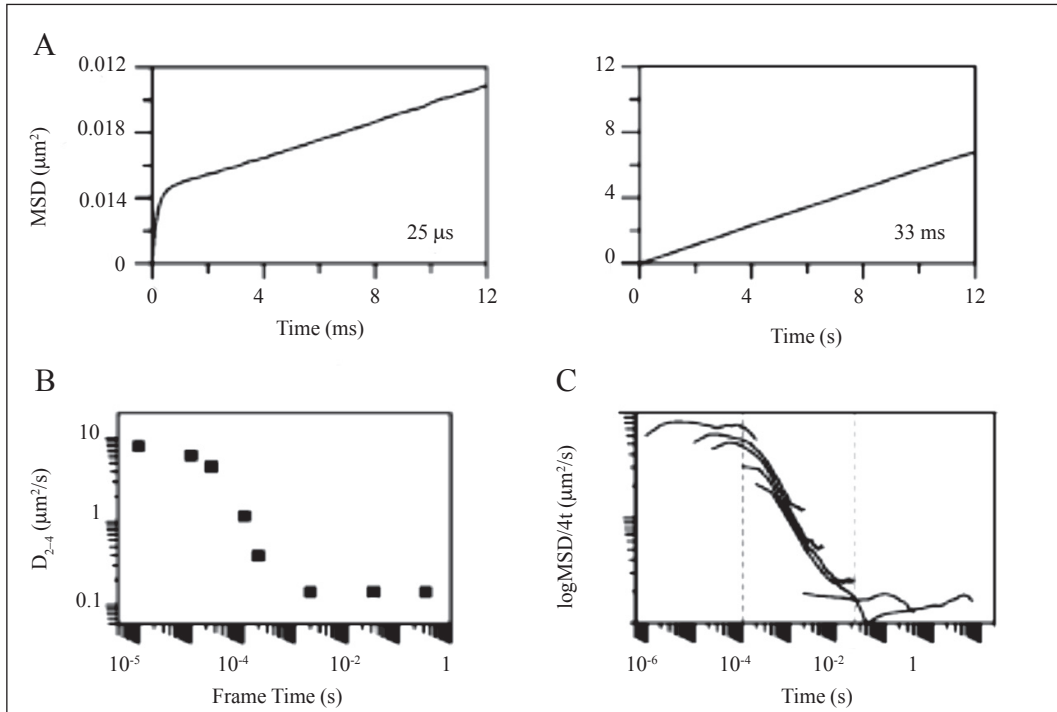


Fig. 1. (A) Mean squared displacements (MSDs) for single trajectories of hop diffusion (those shown in Fig. 5) observed at frame times of 25 ms (left) and 33 ms (right). (B) Apparent microscopic diffusion coefficient D_{2-4} plotted against the frame time (at least 100 simulations for each frame time). The set diffusion coefficient in the simulation was 9 μ m²/s. (C) The plot of $\log(\text{MSD} / \text{time})$ against $\log(\text{time})$, covering six orders of magnitude in time

THE MATHEMATICAL MODEL OF DIFFUSION

The classical rule of diffusion says that the concentration distribution $w(x, t)$ obeys the classical equation of diffusion,

$$W_t = D w_{xx}, \quad (1)$$

in which the coefficient of diffusion is independent of time and coordinate: $D = \text{const}$;

$$w_t \equiv \frac{\partial w}{\partial t}, \quad w_{xx} \equiv \frac{\partial^2 w}{\partial x^2}.$$

The fundamental solution of the diffusion equation is

$$w(x, t) = \frac{Q}{\sqrt{4\pi D(t-t_0)}} e^{-\frac{x^2}{4D(t-t_0)}}, \quad t > t_0, \quad (2)$$

where Q is the total quantity of matter. The Q value is also constant ($Q = \text{const}$), because

$$\int_{-\infty}^{+\infty} \frac{e^{-\frac{x^2}{4Dt}}}{\sqrt{4\pi Dt}} dx = 1. \quad (3)$$

Experimental studies [1] show that the coefficient of diffusion D is not a constant value and depends on the time momentum t : $D = D(t)$. This means that, instead of the classical equation of diffusion (1), we should deal with the equation

$$w_t = D(t) w_{xx} \quad (4)$$

whose properties certainly differ from those of the classical equation of diffusion.

The equation of diffusion with the time-dependent coefficient of diffusion D may be solved analytically. Since the coefficient of diffusion depends only on the time variable t and does not depend on the spatial variable, the dependence of the solution of equation (4) on the spatial coordinate x , as compared with the solution of the classical equation of diffusion (2), should remain the same. In the solution of equation (4), as compared with the solution of equation (2), only the time dependence may change. With this in mind, we shall look for equation (4) solution in the following form:

$$w(x, t) = Q e^{\varphi(t)x^2 + \psi(t)}, \quad (5)$$

where the functions $\varphi(t)$ and $\psi(t)$ are only time-dependent. Substitution of expression (5) into equation (4) gives us two equations:

$$\varphi_t = 4D\varphi^2, \quad \psi_t = 2D\varphi, \quad D = D(t). \quad (6)$$

Both equations may be solved analytically:

$$\varphi(t) = \frac{1}{A - 4 \int D dt}, \quad \psi(t) = B + 2 \int D \varphi dt, \quad (7)$$

where A and B are the integration constants whose values are determined with regard to the initial conditions. Note here that $D(t) > 0$ and $\int D(t) dt > 0$. This means that for some $t = t_0$, $\varphi(t)$ has a singularity.

The simplest way to determine the values of constants A and B is to use the asymptotic expression of solution (5) for $D = \text{const}$:

$$\varphi(t) = \frac{1}{A - 4Dt}; \quad \psi(t) = B - \frac{1}{2} \ln |A - 4Dt|. \quad (8)$$

Substitution of $\varphi(t)$ and $\psi(t)$ according to expressions (7) into solution (5) should furnish the solution (2) of the classical equation of diffusion. This means that the coefficients A and B turn into

$$A = 4Dt_0, \quad B = \ln Q, \quad t > t_0, \quad (9)$$

i. e. constant A depends on the initial moment of time, and constant B is the normalization constant depending on the total quantity of matter Q .

Thus, we have found that the equation of diffusion, with the time-dependent coefficient of diffusion $D(t)$ (4), has the analytical solution (5) with functions $\varphi(t)$ and $\psi(t)$ according to expression (7).

THE PHENOMENOLOGICAL COEFFICIENT OF DIFFUSION

As we see, a concrete solution (5) with the functions (7) of the equation of diffusion (4) depends on the form of the coefficient of diffusion $D(t)$.

The dependence of the coefficient of diffusion revealed in experiments with molecules that undergo non-Brownian diffusion in the plasma membrane [1] is presented in Fig. 1. We shall approximate this step-type dependence by the following function:

$$D(t) = \frac{2h}{\pi} \arctg(b - at) + c, \quad (10)$$

where a , b , c and h are the parameters that determine the form of dependence $D(t)$ (see Fig. 2).

Substitution of the expression $D(t)$ (10) of the coefficient of diffusion into the formulas of the general solution (7) gives

$$\varphi(t) = \left\{ A - 4ct + \frac{8h(b-at)}{a\pi} \arctg(b-at) - \frac{4h}{a\pi} \ln[1 + (b-at)^2] \right\}^{-1}, \quad (11)$$

$$\psi(t) = B - \frac{1}{2} \ln \left| -a\pi A + 4a\pi ct - 8h(b-at) \arctg(b-at) + 4h \ln[1 + (b-at)^2] \right|.$$

These expressions should be substituted into the form (5) of the general solution to obtain the solution of equation (4).

Parameters A and B are determined by the values of the asymptotic solution. Considering that

$$\lim_{t \rightarrow \pm\infty} \int D(t) dt = \pm \frac{bh}{a} + D_{\pm\infty} t, \quad (12)$$

we obtain that if

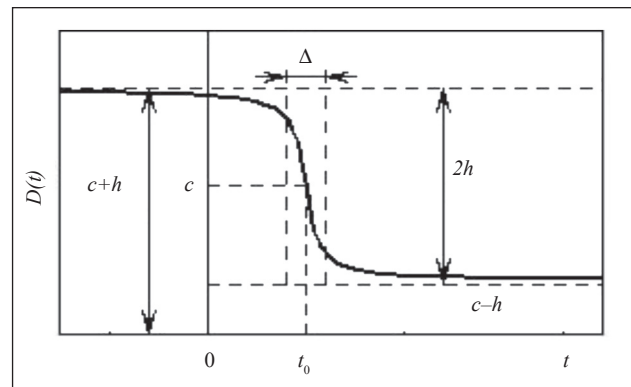


Fig. 2. The step-type time-dependence of the diffusion coefficient $D(t)$; a determines the height of the "step", b modifies the choice of the initial moment ($b = at_0$), while c and h define the asymptotic values; $D_{\pm\infty}$ are the values of the asymptotic coefficient: $D_{\pm\infty} \equiv \lim_{t \rightarrow \pm\infty} D(t) = c \pm h$; $2h$ is the difference among the asymptotic values: $2h \equiv D_{-\infty} - D_{+\infty}$ ("step" height); $\Delta = \frac{2h}{a}$ is the effective width of the step. The a , b , c and h values are determined experimentally

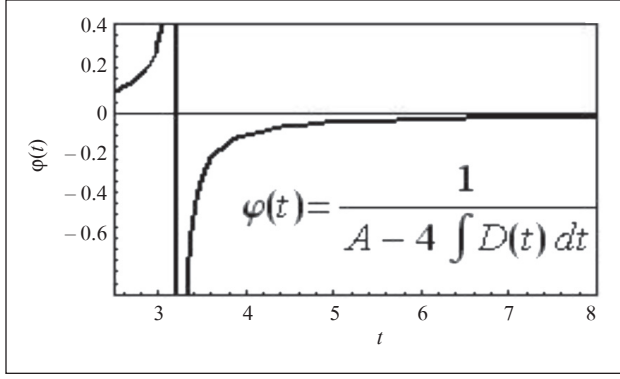


Fig. 3. Dependence of the function $\varphi(t)$ according to the expression (11) for the diffusion coefficient $D(t) = \arctg(10-t) + 2$

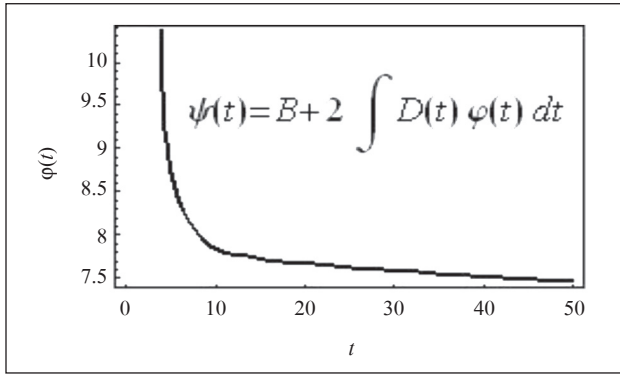


Fig. 4. Dependence of the function $\psi(t)$ according to the expression (11) for the diffusion coefficient $D(t) = \arctg(10-t) + 2$

$$A \equiv 4D_{\infty}t_0 + \frac{4bh}{a}, \quad (13)$$

then

$$\varphi(t) \xrightarrow{t \rightarrow +\infty} \left\{ A - \frac{4bh}{a} - 4(c-h)t \right\}^{-1} \equiv -\frac{1}{4D_{\infty}(t-t_0)}; \quad (14)$$

$$\psi(t) \xrightarrow{t \rightarrow +\infty} B - \frac{1}{2} \ln |4\pi a D_{\infty}(t-t_0)|. \quad (15)$$

From expression (15), if integral (3) is used, it follows that

$$B = \ln(\sqrt{a} Q), \quad (16)$$

where Q is the total constant quantity of matter.

CONCLUSIONS AND DISCUSSION

We have to stress here that the experimentally determined parameters characterizing hop diffusion are severely affected by time-averaging over the frame time, the number of observations made during the residency period within a compartment,

and the total observation time which, if inappropriately chosen, may lead to an erroneous conclusion that the diffusion is simple Brownian.

Note that both x - and y -axes are expanded 1000-fold in Fig. 1 on the right (for 33 ms). At a frame time of 33 ms (right), the plot can be fitted with a linear line showing a simple Brownian character. However, at a frame time of 25 ms, typical hop diffusion characteristics are apparent: a fast rise in the short-time regime and a slower linear growth of MSD with time in the long-time regime, with a slope comparable to that found in the 33-ms MSD-t plot.

At short frame times, the diffusion coefficient within a compartment can be detected with reasonable levels of fidelity. It is clear that at shorter frame times, the diffusion coefficient dominates within a compartment. At much longer frame times, the apparent diffusion coefficient levels off. In this time regime, the diffusion coefficient within a compartment (set at 9 mm²/s) becomes negligible, and the apparent diffusion coefficient is determined by the hop diffusion between the compartments, i.e. the compartment size and the residency time within a compartment.

Note that the time here is not frame time, but the actual time interval of the observation of simulated particles. The individual solid curves are those obtained for each frame time. The vertical broken lines show the time taken to first sense the barriers (at 0.1 ms) and the median residency time within a compartment (at 23 ms). Very clear anomalous diffusion (the best fit for the a -value 0.23, i. e. a slope of 0.77) is observed inbetween these lines, whereas simple Brownian diffusion is observed at time-windows below and above these crossover timescales.

From expressions (14)–(16) we obtain that for $t \rightarrow \infty$ the solution $w(x, t)$ of the corresponding diffusion equation (4) turns into the classical diffusion with the constant diffusion coefficient D_{∞} , and all differences appear at the initial stage of diffusion where the difference between the classical and time-dependent coefficients of diffusion is largest.

As follows from the general form of solution (5) with functions $-\varphi(t)$ and $-\psi(t)$ (7), the analogs of the normalization of integral and the MSD are

$$\int_{-\infty}^{+\infty} e^{-x^2 \varphi(t) - \psi(t)} dx = \sqrt{\pi} \frac{e^{-\psi(t)}}{\sqrt{\varphi(t)}}, \quad \int_{-\infty}^{+\infty} x^2 e^{-x^2 \varphi(t) - \psi(t)} dx = \frac{\sqrt{\pi}}{2} \frac{e^{-\psi(t)}}{\varphi^{3/2}(t)}. \quad (17)$$

From these expressions it follows that the asymptotic behaviour of the MSD $\sim (2\varphi(t))^{-1} = [A - 4 \int D(t) dt]/2$, which coincides with the MSD from Fig. 1A.

An additional result, which follows from the proposed model, is a new form of the normalizable functions:

$$\int_{-\infty}^{+\infty} \frac{\sqrt{\varphi(t)}}{\sqrt{\pi}} e^{-x^2 \varphi(t)} dx = 1 \quad \text{and} \quad (18)$$

$$\int_{-\infty}^{+\infty} x^2 \frac{\sqrt{\varphi(t)}}{\sqrt{\pi}} e^{-x^2 \varphi(t)} dx = \frac{1}{2\varphi(t)} = \frac{1}{2} [A - 4 \int D(t) dt]. \quad (19)$$

Thus, the diffusion model with the time-dependent coefficient of diffusion describes an anomalous diffusion of phos-

pholipids in the compartmentalized cell membrane. The macroscopic size of the diffusing molecules, on the one hand, and the inhomogeneous character of the cell medium on the other serve as a theoretical basis for modifying the available models of transport. In author's opinion, these two important circumstances provide a sufficient reason for refining Fick's law:

$$j = -D(t)c_x; \quad c_t = j_x. \quad (20)$$

In this approach, as a consequence, also the mathematical model of the diffusion process (see, e. g., [11, 12]) should be changed correspondingly:

$$c_t = D(t)c_{xx}. \quad (21)$$

Note here that dependence $D = D(x)$ or $D = D(x, t)$ does not obey equation (20). In other words, equation

$$c_t = D(x, t)c_{xx}$$

does not describe any diffusion, contrary to the, unfortunately, very popular error.

The proposed model of diffusion essentially differs from other models of this kind, among them most popular being:

a) classical diffusion: $c_t = Dc_{xx}, |c_x| \ll 1, D = \text{const}(x, t)$ (13)

b) nonlinear diffusion: $c_t = [D(c)c_x]_x, \lim_{x \rightarrow x_0} D(c) = \text{const}$ (14);

c) nonlocal diffusion: $c_t = Dc_x^{(1+\alpha)}, j = -Dc_x^{(\alpha)}$, where $c_x^{(\alpha)}$ is the fractional derivative of the order α [11, 12].

The proposed model differs from them not only by the behaviour of the corresponding solutions, but also by the dependence of the MSD in respect of time. This value, as a rule, may be observed experimentally and its behaviour may be a decisive factor while choosing one or another model of diffusion.

References

1. Ritchie K, Shan X-Y, Kondo J, Iwasawa K, Fujiwara T, Kusumi A. *Biophys J* 2005; 88: 2266–77.
2. Murase K, Fujiwara T, Umemura Y, Suzuki K, Iino R, Yamashita H, Saito M, Murakoshi H, Ritchie K, Kusumi A. *Biophys J* 2004; 86: 4075–93.
3. Fujiwara T, Ritchie K, Murakoshi H, Jacobson K, Kusumi A. *J Cell Biol* 2002; 157: 1071–81.
4. Smith PR, Morrison IEG, Wilson KM, Fernandez N, Cherry RJ. *Biophys J* 1999; 76: 3331–44.
5. Saxton MJ. *Biophys J* 1996; 70: 1250–62.
6. Tomishige M, Sako Y, Kusumi A. *J Cell Biol* 1998; 142: 989–1000.
7. Sako Y, Kusumi A. *J Cell Biol* 1994; 125: 1251–64.
8. Sako Y, Nagafuchi A, Tsukita S, Takeichi M, Kusumi A. *J Cell Biol* 1998; 140: 1227–40.
9. Kusumi A, Sako Y, Fujiwara T, Tomishige M. *Methods Cell Biol* 1998; 55: 173–94.
10. Iino R, Koyama I, Kusumi A. *Biophys J* 2001; 80: 2667–77.
11. Miškinis P. *Nonlinear and Nonlocal Integrable Models*. Vilnius: Technika, 2003.
12. Miškinis P. *Biology* 2005; 4: 156–9.
13. Landau LD, Lifshitz EM, *Statistical Physics (Course of Theoretical Physics, V. 5)* Butterworth-Heinemann, 1984.
14. Samarskij AA, Nikolaev ES. *Numerical Methods for Grid Equations*. Vol. I Basel: Birkhäuser, 1988.

Paulius Miškinis

ANOMALI FOSFOLIPIDŲ SUBDIFUZIJA SEKCIONUOTOJE LĄSTELĖS MEMRANOJE IR MATEMATINIS DIFUZIJOS MODELIS SU NUO LAIKO PRIKLAUSANČIU DIFUZIJOS KOEFICIENTU

Santrauka

Eksperimento metu, analizuojant fosfolipidų difuziją sekcionuotoje ląstelės membranoje, pastebėtas nuokrypis nuo klasikinės difuzijos. Pasiūlytas naujas matematinis modelis su nuo laiko priklausančiu difuzijos koeficientu. Nagrinėjamas konkretus šio modelio taikymas su laiptelio tipo asimptotinė difuzijos koeficiento priklausomybe bei aptartas jo ir eksperimentinių rezultatų atitikimas. Atsitiktinis nejudančių sklaidos centrų pasiskirstymas ląstelėje, taip pat membranos skeleto tinkelis gali sudaryti teorinę prielaidą modifikuoti atitinkamą transporto modelį ir atitinkamą difuzijos lygtį. Rezultatai rodo, kad eksperimento metu gauta difuzijos koeficiento priklausomybė nuo laiko derinasi su straipsnyje pasiūlytu teoriniu modeliu.